Spatial-temporal analysis of tuberculosis infections in a rural prefecture in Japan

Yixiao Lu [1], Guoxi Cai [1,2,3], Kazuhiko Arima [1], Fei He [4], Zejun Zheng [5], Liang Qin [3], Kiyoshi Aoyagi [1*]

1. Department of Public Health, Nagasaki University Graduate School of Biomedical Sciences, Nagasaki, 852-8523, Japan;
2. Public Health and Hygiene Research Department, Nagasaki Prefectural Institute of Environment and Public Health, Nagasaki 856-0026, Japan;
3. Department of International Health and Medical Anthropology, Institute of Tropical Medicine (NEKKEN), Nagasaki University, Nagasaki, 852-8523,Japan;
4. Department of Epidemiology and Health Statistics, Fujian Provincial Key Laboratory of Environment Factors and Cancer, School of Public Health, Fujian Medical University, Fuzhou 350122, Fujian, China;
5. Graduate School of Fisheries and Environmental Sciences, Nagasaki University, 852-8521, Japan;

Background: Japan has remained medium-burden tuberculosis (TB) country for many years. However, a considerable variation was observed in the TB space-time distribution among Japan's eight regions. This study aimed to investigate the spatial, temporal, and space-time dynamics of TB at the *machi*-level in Nagasaki prefecture.
Methods: Data on the reported TB infections from 2007 to 2018 were collected from the information center for infectious diseases of the Nagasaki Prefectural Institute of Environment and Public Health. The time series, temporal trends, and spatial patterns of TB at the *machi*-level were explored using Moran's I and Kulldorff's space-time scan statistics.
Results: A total of 4,364 TB infections were reported between April 2007 and December 2018 in Nagasaki prefecture. The infections were frequently reported in October, June, and January, and they showed spatial clustering with Moran's I value ranging from 0.07 to 0.17 (p = 0.001). Ten significant clusters were identified, including one most likely cluster and nine secondary clusters, which were mainly concentrated in the densely inhabited districts of the two biggest cities in Nagasaki prefecture (Nagasaki city and Sasebo city), Shimabara peninsula, and Iki island.
Conclusion: This study showed significant and unique spatial-temporal characteristics of TB infections in Nagasaki prefecture. Therefore, such information on the prevailing epidemiological situation of TB infections could help develop strategies that could effectively eliminate TB in Japan.

Introduction

Tuberculosis (TB) is an infectious disease caused by bacillus *Mycobacterium tuberculosis* (*M. tuberculosis*), which generally results in pulmonary TB (PTB) as well as extrapulmonary TB (1). TB is one of the top 10 causes of death worldwide. In 2017, an estimated 10 million TB infections occurred, and 1.6 million TB-related fatalities were reported (2). To achieve the goal of eliminating TB, the World Health Organization launched the "End TB Strategy," which aims at reducing the TB incidence to less than 10 new tuberculosis cases per 100,000 people per year and a 95% decrease in TB deaths by 2035 (3).

As a medium-burden TB country, the Ministry of Health, Labour and Welfare of Japan (MHLW) has been committed to promoting international cooperation to fight TB; it also enhanced its national TB control program through the announcement of the "Stop TB Japan Action Plan" (4) in 2008 and initiation of the "Stop TB Japan" (5) in 2015. The TB notification rates in Japan have significantly decreased since

1980; however, the incidence of TB increased among the older population (6,7), the younger population (8), and the foreign-born population from high-burden TB countries (9). A considerable variation in TB distribution exists among Japan's eight regions. According to the Japan Tuberculosis Surveillance Center's "Annual Report 2018" (10), the Kinki region had the highest notification rate (17.2 per 100,000 people), while the Tohoku region had the lowest notification rate (8.3 per 100,000 people).

Several studies evaluating the spatial and temporal distribution of TB have reported the highly complex dynamics and spatially heterogeneous (national and provincial) distribution of TB infection in different periods; however, the variations in small regions are often neglected in such large-scale analysis (11–13). The Kulldorff's space-time scan statistical method can detect the distribution characteristics in temporal and spatial axes, thus reflecting the real-world scenarios (14). This method has been applied to detect infectious disease hotspots in recent years (15,16); in terms of identifying TB clusters, meaningful results were obtained (17,18). A better understanding of the spatial epidemiology of TB could help policymakers and different stakeholders to formulate effective prevention and control strategies (19,20). Thus, the analysis of TB situations at the first administrative level, then moving to a smaller administrative level, could help in the implementation of appropriate and sustainable plans to eliminate TB. Japanese administration is divided into three basic levels; national, prefectural, and municipal. The municipal divisions are subdivided into cities, towns, and villages; municipal boundary areas are determined by the local public and called "*machi*" in this study.

A few studies have explored the spatial epidemiology of TB at a fine scale in rural areas of Japan. Therefore, this study aimed to investigate the spatial, temporal, and space-time dynamics of TB at the *machi*-level in Nagasaki prefecture.

Materials and Methods

Ethics approval and consent for participation

This study was approved by the Research Ethics Committees of Nagasaki Prefectural Institute of Environment and Public Health (No. 2021-9-1). This study did not include any human subjects, and the patient records were anonymized and de-identified before the analysis. The study was conducted according to the guidelines of the Declaration of Helsinki. The need of informed consent was waived by the Nagasaki Prefectural Institute of Environment and Public Health ethics committee.

Study setting and data sources

Nagasaki prefecture is located on the island of western Kyushu and consists of four peninsulas centered around Omura Bay (Kitamatsuura, Nishisonogi, Nagasaki, and Shimabara) and three remote islands (Tsushima, Iki, and Goto). The Nagasaki prefecture comprises 13 cities and 8 towns/villages (Figure 1), with a total population of 1.3 million people in 2018. According to the 2015 national census data, there are a total of 1,943 *machis* in Nagasaki prefecture; the most populated *machi* is Nameshi in Nagasaki City (12,775 people), and the median population is 377.5 people. 77 *machis* contain 0 people due to a lack of data from the 2015 national census.

Data on the reported TB infections were extracted from the information center for infectious diseases of the Nagasaki Prefectural Institute of Environment and Public Health. A total of 4,364 TB infections were notified in Nagasaki prefecture from April 2007 to December 2018. An epidemiological analysis of the 12-year TB data was performed in a previous study (21). In this study, using the registration date of TB infection and the spatial location information in the TB dataset, 4,364 TB infections were assigned to the appropriate *machi*. The data aggregated at the *machi*-level monthly were used to detect the spatio-temporal high-risk areas. The *machi*-level Nagasaki prefecture population data from 2015 and shapefile maps of Nagasaki prefecture used in this study were downloaded from e-Stat (a portal site for Japanese Government Statistics) (http://www.e-stat.go.jp/en).

Statistical analysis

The global Moran's I was used to measure whether the reported TB infections from *machi* in Nagasaki prefecture are affected by the neighboring regions (22). The global Moran's I value ranging from −1 to 1 was used to detect the degree of spatial autocorrelation of research object from the whole region, while Moran's I value equal to 0 indicates no spatial clustering (23).

The Kulldorff's space-time scan statistic method implanted in SaTScan™ v9.6 software (www.satscan.org/) was used to detect the temporal, spatial, and space-time clusters of TB infections (24). The potential clusters are the areas with high TB notification rates that significantly exceeded the TB notification rates of nearby regions (p < 0.05). Since the TB notification rate was not very high, the discrete Poisson probability model was used for scanning (25).

The null hypothesis H_0 stipulates that the model describes a constant risk of TB infection with an intensity μ (proportional to the at-risk population). By contrast, the alternative hypothesis
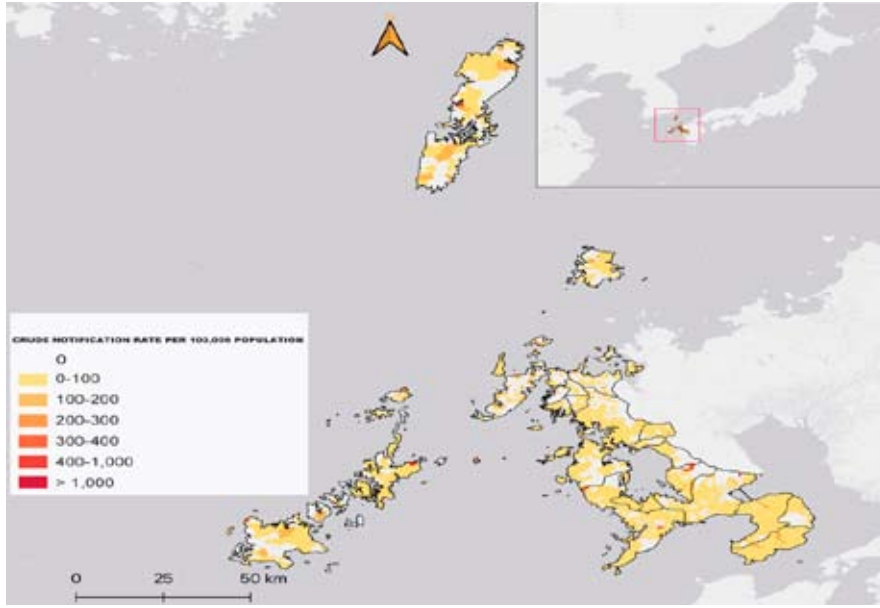
Figure 1. The average annual crude notification rate of TB infections (per 100,000 population) in Nagasaki prefecture, from April 2007 to December 2018

H_A supports that the number of observed cases is more than the expected cases. The expected number of TB infections was calculated using Equation (1): $\mu = P * C / p$ (p: population in a geographic area (*machi*); C: the total number of TB infections; P: the total population in Nagasaki prefecture). The cluster is identified using the likelihood ratio (*LLR*) test in Equation (2):

$$(2) \quad \frac{L(Z)}{L_O} = \frac{\left(\frac{n_z}{\mu(Z)}\right)^{n_z} \left(\frac{N - n_Z}{N - \mu_{(Z)}}\right)^{N - n_z}}{\left(\frac{N}{\mu(T)}\right)^{N}}$$

(n_z: the number of cases inside the cylinder n_z; $\mu(Z)$: the expected number of cases in cylinder Z; N: ; the number of observed cases for the entire study area during the entire study period; $\mu(T)$: the total number of expected cases in the study area across all time). Risk is elevated for the cylinder with a likelihood ratio greater than 1.

The potential cluster with the maximum likelihood ratio was defined as the most likely cluster, while the rest of clusters with statistically significant *LLR* were defined as the secondary clusters (p < 0.05). The p-value of *LLR* was estimated using 999 Monte Carlo simulations (26). The space-time scan statistics were used to calculate the infinite number of discrete, cylindrical windows with a circular geographic base and height corresponding to time (27). Each cylindrical window was evaluated as a possible TB infection space-time cluster.

The relative risk (*RR*) of TB in each cluster was calculated

to evaluate the risk of TB in the clustered areas (28) using Equation (3):

$$(3) \quad RR = \frac{c / e}{(C - c)/(C - e)}$$

(c: the total number of cases in a cluster; e: the number of expected cases in a cluster; C: the total number of observed cases in the Nagasaki prefecture).

TB data from 2007 were used to determine the spatial scanning windows by increasing the cluster size from 4% to 50% of the population at risk; the value was restricted to 50% to identify no overlap in candidate clusters and cover the largest high-incidence geographic areas as much as possible (29). The TB data from 2007 to 2011 were used to determine the temporal scanning window set. For the same reason, a maximum temporal cluster size of 50% of the total study period was set. Furthermore, each candidate cluster must include at least two cases and have a minimum duration of 2 days. The previous study found a significant difference in the distribution of TB infections in terms of sex and age; therefore, these variables were used as covariate variables for covariate adjustment in the retrospective space-time scan statistics.

Additionally, the time-series analysis based on the additive decomposition model was used to estimate the seasonal effects on the reported TB infections in Nagasaki prefecture from 2007 to 2018 (30): Xt = seasonal (St) + trend (Tt) + random, where Xt is the number of TB infections, and t is the time in the unit of the month.

All statistical analyses were performed using RStudio version 1.4.1717 (31); the spatial autocorrelation analysis was applied using the spdep R package (32); the choropleth maps representing the detected disease clusters were created using QGIS 3.20.2-Odense.

Results

A total of 4,364 TB infections were included in this study. 1206/1943 *machis* in Nagasaki prefecture have reported at least one case of TB infection. The average annual crude notification rate of TB infections (per 100,000 population) at the *machi*-level in Nagasaki prefecture from April 2007 to December 2018 is shown in Figure 1. The average annual crude notification rate across the 12 years of data reviewed for this study ranged from 2.15 to 2083.33 per 100,000 population.

Temporal pattern of reported TB infection

The time-series analysis based on the additive decomposition model of TB infections indicated slightly upward and downward trends between 2007 and 2013, followed by a sudden increase until early 2014, a decrease in mid-2014 and mid-2015, and a slowly increasing trend after 2015 (Figure 2a: trend). TB infection had no apparent periodicity seasonality and seasonal effects between 2007 and 2018 (Figure 2b). Nevertheless, two vague seasonal patterns were shown from 2007 to 2011 and between 2013 and 2017 (Figure 2a: seasonal). The maximum seasonal index values were 1.15 in October, 1.14 in June, and 0.83 (the lowest value) in January (Figure 2c).

The temporal cluster analysis identified four significant temporal clusters in 2007, 2008, 2011, and 2014 (Table 1). The temporal cluster analysis showed that TB infection occurred sporadically in the autumn, winter, and early spring from September to mid-March. The highly aggregated period for TB was from February 20, 2014 to March 19, 2014, with 84 reported TB cases (*LLR* =36.9, p = 0.001).
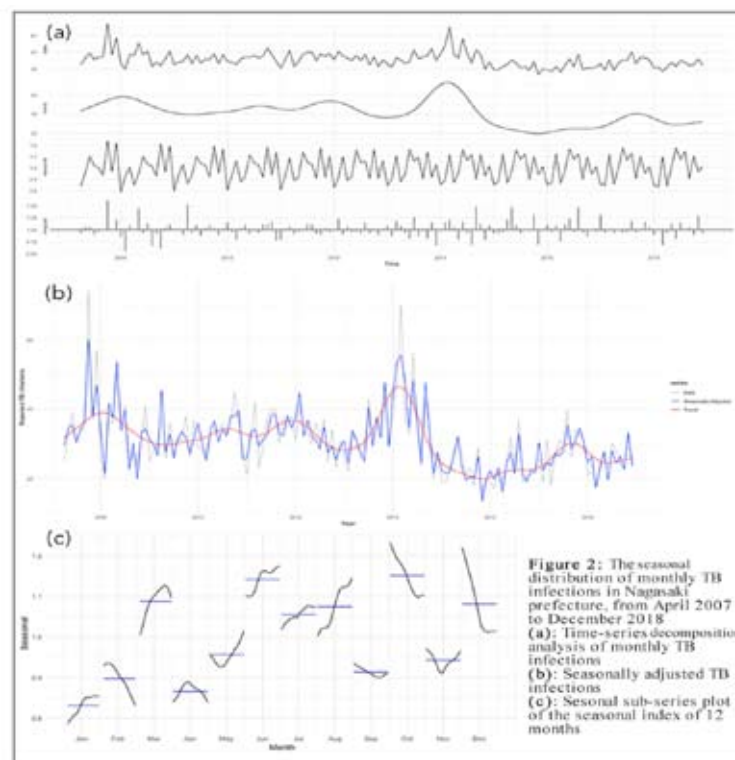

Figure 2. Seasonal distribution of monthly TB infection in Nagasaki prefecture, from April 2007 to December 2018
(a) The monthly TB infections are decomposed into three parts: trend, seasonal and irregular; (b) The blue line shows the time-series TB infections adjusted for seasonal effect. The grey and red lines are the non-adjusted time-series TB infections and trends from (a); (c) The seasonal index is calculated for each month. The blue and black lines show the average seasonal index and the yearly seasonal index of each month, respectively.

Table 1. Temporal clustering of TB infection in Nagasaki prefecture from April 2007 to December 2018

Year	Cluster time frame	Duration (day)	Observed cases	Expected cases	RR	LLR	p-value
2007	October 18, 2007 to October 19, 2007	2	21	2.66	8.31	25.51	0
2008	November 25, 2008 to December 5, 2008	11	31	11.93	2.73	11.01	0.01
2011	September 16, 2011 to September 16, 2011	1	8	1.11	7.35	8.98	0.02
2014	February 20, 2014 to March 19, 2014	26	84	36.44	2.59	25.27	0
All year	February 20, 2014 to March 19, 2014	26	84	27.87	3.05	36.9	0

The non-significant (p-value ≥ 0.05) temporal clustering results are not shown in Table 1 (2009, 2010, 2012, 2013, 2015, 2016, 2017, 2018)

Spatial pattern of reported TB infections

The annual global Moran's I value at the *machi*-level indicated a positive spatial autocorrelation in Nagasaki prefecture, ranging from 0.07 to 0.17 (p = 0.001). The spatial clustering analysis of 12 years identified five significant spatial clusters, covering 215 *machis* in Nagasaki prefecture (Table 2). The most likely cluster was identified in T-*machi* in Nagasaki city (*LLR* = 59.72, p < 0.001); the secondary clusters were identified near Nagasaki port and Sasebo port, in the Shimabara peninsula, and A-*machi* in remote Goto island. The notification rate of TB infection inside the cluster areas was higher than that in the areas outside.

Spatio-temporal pattern of TB infection

Figure 3 shows the spatio-temporal clusters of TB infection in Nagasaki prefecture using retrospective space-time scan statistics. Ten significant clusters were identified, including one most likely cluster and nine secondary clusters. The clusters are distinguished in different colors in Figure 3, and the characteristics of these clusters are summarized in Table 4. The most likely cluster was identified in T-*machi* in Nagasaki city, with 34 reported TB cases, and the high-risk period was from September 1 to December 31, 2007 (*LLR* = 167.81, p < 0.001). The secondary clusters were identified in Nagasaki city, Sasebo city, Shimabara peninsula, Goto island, and Iki island.

The secondary clusters from Nagasaki city and Sasebo city were identified in the densely inhabited districts (DIDs) (33) in those two primary cities of Nagasaki prefecture. In addition, five spatio-temporal clusters containing just one *machi* were detected (including the most likely cluster). The four secondary clusters (containing a single *machi*) occurred in 2013 and 2014 in less than 2 months; the relative risk of these secondary clusters was extremely high (varying from 343.49 to 589.46). The cluster with the most extended duration (secondary cluster 3) was detected in the Shimabara peninsula, including almost the entire Unzen city and Minamishimabara city.

Table 2. Spatial clustering of TB infection in Nagasaki prefecture from April 2007 to December 2018

Cluster type	Radius (km)	Observed cases	Expected cases	Relative Risk	p-value	*Machi* (total)	Population
Most likely cluster	0	39	3.4	11.57	<0.001	1	995
Secondary cluster 1	10.2	351	198.88	1.83	<0.001	70	63,040
Secondary cluster 2	2.08	265	150.4	1.81	<0.001	38	49,983
Secondary cluster 3	1.85	273	191.81	1.45	<0.001	105	64,246
Secondary cluster 4	0	8	0.63	12.68	0	1	124

The spatial cluster with a 0 km Radius indicates only one *machi* is included in the cluster; a Relative Risk greater than 1 indicates higher risk of TB infection for *machis* inside the cluster than *machis* outside the cluster; the Population is the total population included within the cluster.

Table 3. Global Moran's index of TB infection in Nagasaki prefecture from April 2007 to December 2018

Year	Moran's I	z-score	p-value
2007	0.08	7.12	0
2008	0.08	5.17	0
2009	0.08	5.32	0
2010	0.13	8.53	0
2011	0.17	11.39	0
2012	0.14	9.14	0
2013	0.11	7.47	0
2014	0.14	9.64	0
2015	0.08	5.07	0
2016	0.1	6.61	0
2017	0.07	4.54	0
2018	0.07	4.47	0

The Global Moran's I measures spatial autocorrelation using feature locations and values simultaneously. The Moran's I indicates the degrees of clustering of similar values of adjacent *machis*, a z-score greater than 2.58 suggests that there is less than 1-percent likelihood that the clustered pattern is a result of random chance.
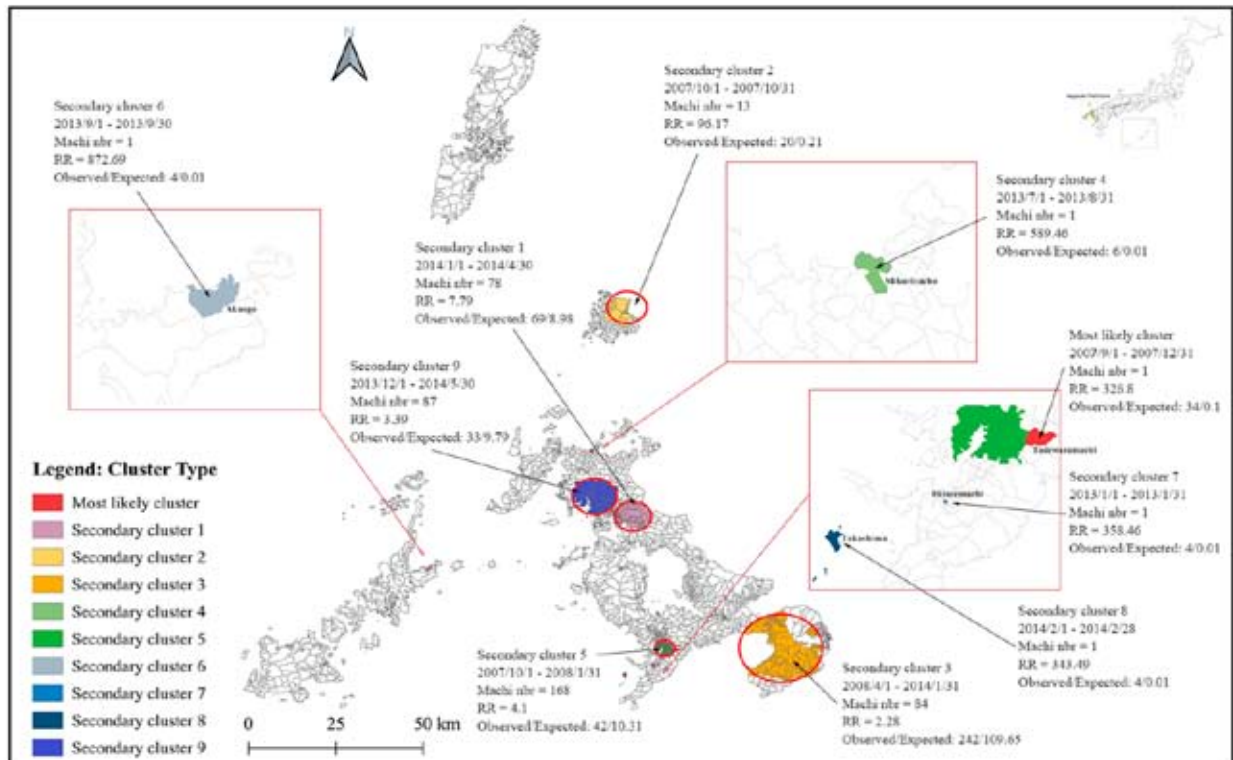

Figure 3. Spatio-temporal clustering of TB infection at the *machi*-level in Nagasaki prefecture, from April 2007 to December 2018 The *machis* included in each detected space-time cluster are shown and distinguished by different colors, additional information for each cluster including period, number of *machi*, relative risk, and the ratio of observed cases and expected cases are annotated.

Table 4. Spatial-temporal clustering of TB infection in Nagasaki prefecture from April 2007 to December 2018

Cluster type	Time frame	Duration (day)	Radius (km)	Observed cases	Expected cases	Relative risk	p-value	*Machi* (total)	Population
Most likely	Sep 1 to Dec 31, 2007	121	0	34	0.1	326.8	<0.001	1	1,026
SC 1	Jan 1 to April 30, 2014	119	5.19	69	8.98	7.79	<0.001	78	105,073
SC 2	Oct 1 to Oct 31, 2007	30	5.57	20	0.21	96.17	<0.001	13	7,954
SC 3	April 1, 2008 to Jan 31, 2014	2131	11.84	242	109.65	2.28	<0.001	84	64,728
SC 4	July 1 to Aug 31, 2013	61	0	6	0.01	589.46	<0.001	1	210
SC 5	Oct 1, 2007 to Jan 1, 2008	122	2.84	42	10.31	4.1	<0.001	168	110,713
SC 6	Sep 1 to Sep 30, 2013	29	0	4	0.01	872.69	<0.001	1	132
SC 7	Jan 1 to Jan 31, 2013	30	0	4	0.01	358.46	<0.05	1	576
SC 8	Feb 1 to Feb 28, 2014	27	0	4	0.01	343.49	<0.05	1	382
SC 9	Dec 1, 2013 to June 30, 2014	211	6.27	33	9.79	3.39	<0.05	87	69,941

Most likely: the most likely cluster; SC: secondary cluster

The spatial-temporal cluster with a 0 km Radius indicates only one *machi* is included in the cluster; a Relative Risk greater than 1 indicates higher risk of TB infection for *machis* inside the cluster than *machis* outside the cluster; the Population is the total population included within the cluster.

Discussion

This study analyzed the spatial-temporal situation of the reported TB infections from 2007 to 2018 in Nagasaki prefecture using the smallest administrative unit on the *machi-*level scale. This study was the first to investigate the status of TB infections at the machi-level in a rural prefecture with a relatively high TB notification rate in Japan. Our study demonstrated a significant space-time clustering in the distribution of TB infections in Nagasaki prefecture. The high-risk areas were mainly concentrated in the DIDs of Nagasaki city and Sasebo city, the two biggest cities in Nagasaki prefecture, Shimabara peninsula, and Iki island. Temporal clustering was sporadic in the autumn, winter, and early spring from September to mid-March.

The Kulldorff's retrospective scan statistics could take multiple factors into account, making it a helpful cluster detection technique for evaluating the geographical and temporal distribution using routinely collected data (25). In the case of TB, public health officials are required to evaluate local disease indicators, it is of significant importance to distinguish the cluster alarms needed further investigation from those that are likely to occur by chance. Moreover, the systemic utilization of cluster detection is essential in the TB control programs by providing information on the spatial-temporal status of TB incidence (34), showing usefulness in the detection of clusters of designated diseases in a range of

settings and identification of factors behind the spread of the diseases. Therefore, to help guide the provision, planning, and optimization of TB control strategies.

In this study, a total of 4,364 TB infections were notified between April 2007 to December 2018 in Nagasaki prefecture; the majority of reported TB were older than 65 years, and the notification rate in older adults was extremely high, especially in men aged >85 years (21). The findings of our study showed no apparent periodicity seasonality; the seasonal index value indicated that the registration peak months of TB infections were June and October. Meanwhile, the temporal cluster analysis identified a high-risk period for TB infections in 2007, 2008, 2011, and 2014, mainly occurring from September to mid-March, specifically, October 18 to 19 in 2007, November 25 to December 5 in 2008, on September 16 in 2011, and February 20 to Mach 19 in 2014. A study on the periodic structures of active TB in Japan (8) reported that the TB epidemic in individuals aged ≥70 years occurred in August and September, while that in individuals aged 10–39 years occurred in June and July. Environmental conditions such as increased time of indoor activities (35) and vitamin D deficiency due to limited exposure to sunlight (36, 37), and biological factors such as seasonal immunocompetence (38) were related to the seasonality of TB infections. Another study suggested that health checkups in young adults, reactivation of latent TB infection due to aging, and lifestyle habits in older adults might influence the seasonality of TB incidence

in Japan (39).

The results obtained in this study show a dramatic upward followed by a downward trend in TB infections between 2013 and 2016. No such trend was observed in other time intervals. The highest TB infection was reported in early 2014, while the lowest TB infection was reported in 2015. A possible explanation for this is that TB outbreaks occurred in this period. Hence, further investigation, including molecular genotyping of *M. tuberculosis*, is needed.

Compared with the spatial and temporal scanning models, the time-space scanning could make a more real-world-related conclusion (29). The retrospective space-time scan statistics identified one most likely cluster and nine secondary clusters in this study. The most likely cluster was identified in T-*machi* within Nagasaki city, a typical less populated suburban area consisting of relatively stable inhabitants and equipped with clinics, social welfare centers, schools, etc. The two secondary clusters identified in Sasebo city shared similar living conditions. Secondary clusters 1, 5, and 7 were identified in the DIDs within Nagasaki city and Sasebo city; they are widely known as port or coastal cities, with relatively mass population mobility and more migrant workers or foreigners. Another type of cluster was detected in the remote or offshore islands (secondary clusters 2, 6, and 8); these areas are sparsely populated but have seasonal tourists. A significant proportion of TB from these areas was aged under 65 years. The cluster with the most extended duration (secondary cluster 3) was detected in the Shimabara peninsula, a popular hot spring and hiking destination. The continuous report of TB infections from 2008 to 2014 could be due to regular annual health check-up reports or introduction from outside by seasonal tourism. Further molecular investigation regarding the spreading strains of TB and MDR/SDR-TB is needed.

The TB incidence in the older population has already become a crucial global health problem (40). The incidence of TB among older adults in Japan is extremely high compared with that in other age groups (39). A similar notification rate of TB infections was reported in Nagasaki prefecture (21). After initially implementing the international control TB program ("Stop TB Japan Action Plan") in 2008, MHLW further released the "Stop TB Japan" (4) in 2015. This approach re-addresses priorities and adjusts measures to extensively screen and treat people with latent TB, especially for high-risk groups (older adults, immigrants, etc.); restructure the medical provision system; reinforce TB control in mega-cities. In Japan, TB is primarily detected during regular health checkups among schoolchildren and workers, which is regulated by the Industrial Safety and Health Act (41). However,

the fixed timing of annual health checkups could cause problems like delays in healthcare seeking (42) and non-detection of TB cases during regular screening. Therefore, the provision of geographical information on TB infections on a small scale could help adopt appropriate measures for the early diagnosis of TB among high-risk populations.

Although our study demonstrated the usefulness of spatial and temporal clustering analysis, several limitations were observed. First, the power of cylindrical scan statistics could be limited in some irregular and complex geography. Second, the factors associated with the high-risk clustering, such as socioeconomic factors, were not assessed. Third, the recent transmission was not distinguished from the reactivation of latent TB due to the lack of laboratory evidence. Hence, we hope to improve our findings by conducting further molecular-based studies.

Conclusion

This study analyzed the spatial, temporal, and space-time clusters of TB infection at the *machi*-level in Nagasaki prefecture from April 2007 to December 2018. Results showed significant and unique spatial-temporal characteristics of TB infection in the region. Therefore, using existing data, such information on the prevailing epidemiological situation of TB infection could help in the development of strategies to effectively eliminate TB in Japan.

Conflict of interest

The authors declare that they have no competing interests.

Funding

References

1. Organization WH. Global tuberculosis report 2019. World Health Organization; 2019.

2. Tuberculosis (TB) [Internet]. [cited 2021 Mar 25]. Available from: https://www.who.int/news-room/fact-sheets/detail/tuberculosis

3. Uplekar M, Weil D, Lonnroth K, et al. WHO's new End TB Strategy. *Lancet* 385(9979):1799–801, 2015.

4. Action Plan(F).pdf [Internet]. [cited 2022 Jun 10]. Available from: http://www.stoptb.jp/dcms_media/other/Action%20Plan(F).pdf

5. Stop TB Japan.pdf [Internet]. [cited 2022 May 22]. Available from: https://www.mhlw.go.jp/stf/shingi/2r985200000125vv-att/2r9852000001288b.pdf

6. Hagiya H, Koyama T, Zamami Y, et al. Trends in incidence and mortality of tuberculosis in Japan: a population-based study, 1997-2016. *Epidemiol Infect* 9:1–10, 2018.

7. Ohmori M, Ishikawa N, Yoshiyama T, Uchimura K, Aoki M, Mori T. Current epidemiological trend of tuberculosis in Japan. *Int J Tuberc Lung Dis* 6(5):9, 2002.

8. Kohei Y, Sumi A, Kobayashi N. Time-series analysis of monthly age-specific numbers of newly registered cases of active tuberculosis in Japan from 1998 to 2013. *Epidemiol Infect* 144(11):2401–14, 2016.

9. Kawatsu L, Uchimura K, Izumi K, Ohkado A, Ishikawa N. Profile of tuberculosis among the foreign-born population in Japan, 2007–2014. *Western Pac Surveill Responses J* 7(2):7–16, 2016.

10. Tuberculosis Surveillance Center (2018). Tuberculosis in Japan - annual report 2018. Department of Epidemiology and Clinical Research, the Research Institute of Tuberculosis: Tokyo, Japan. 2018;68.

11. Areias C, Briz T, Nunes C. Pulmonary tuberculosis space–time clustering and spatial variation in temporal trends in Portugal, 2000–2010: an updated analysis. *Epidemiol Infect* 143(15):3211–9, 2015.

12. Cao K, Yang K, Wang C, et al. Spatial-Temporal Epidemiology of Tuberculosis in Mainland China: An Analysis Based on Bayesian Theory. *Int J Environ Res Public Health* 13(5):469, 2016.

13. Middelkoop K, Bekker LG, Morrow C, Zwane E, Wood R. Childhood tuberculosis infection and disease: a spatial and temporal transmission analysis in a South African township. *S Afr Med J* 99(10):738–43, 2009.

14. Kulldorff M, Nagarwalla N. Spatial disease clusters: Detection and inference. *Statistics in Medicine* 14(8):799–810, 1995.

15. Chong S, Nelson M, Byun R, Harris L, Eastwood J, Jalaludin B. Geospatial analyses to identify clusters of adverse antenatal factors for targeted interventions. *Int J Health Geographics* 12(1):46, 2013.

16. Métras R, Porphyre T, Pfeiffer DU, et al. Exploratory Space-Time Analyses of Rift Valley Fever in South Africa in 2008–2011. *PLoS Negl Trop Dis* 6(8):e1808, 2012.

17. Dangisso MH, Datiko DG, Lindtjørn B. Spatio-Temporal Analysis of Smear-Positive Tuberculosis in the Sidama Zone, Southern Ethiopia. *PLoS ONE* 10(6):e0126369, 2015.

18. Hassarangsee S, Tripathi NK, Souris M. Spatial Pattern Detection of Tuberculosis: A Case Study of Si Sa Ket Province, Thailand. *Int J Environ Res Public Health* 12(12):16005–18, 2015.

19. Maciel ELN, Pan W, Dietze R, et al. Spatial patterns of pulmonary tuberculosis incidence and their relationship to socio-economic status in Vitoria, Brazil. *Int J Tuberc Lung Dis* 14(11):1395–402, 2010.

20. Musenge E, Vounatsou P, Collinson M, Tollman S, Kahn K. The contribution of spatial analysis to understanding HIV/TB mortality in children: a structural equation modelling approach. *Glob Health Action* 2013;6:10.3402/gha.v6i0.19266.

21. Lu Y, Cai G, Liu Y, He F, Aoyagi K. Epidemiological Features of Tuberculosis Infection in a Rural Prefecture of Japan from 2007 to 2018. 2022; [Manuscript submitted for publication]. Department of Public Health, Nagasaki University Graduate School of Biomedical Sciences.

22. Thompson ES, Saveyn P, Declercq M, et al. Characterisation of heterogeneity and spatial autocorrelation in phase separating mixtures using Moran's I. *J Colloid Interface Science* 513:180–7, 2018.

23. Moran PAP. Notes on Continuous Stochastic Phenomena. *Biometrika* 37(1/2):17–23, 1950.

24. Jones SG, Kulldorff M. Influence of spatial resolution on space-time disease cluster detection. *PLoS ONE* 7(10):e48036, 2012.

25. Alemu K, Worku A, Berhane Y. Malaria infection has spatial, temporal, and spatiotemporal heterogeneity in unstable malaria transmission areas in Northwest Ethiopia. *PLoS ONE* 8(11):e79966, 2013.

26. Abbas T, Younus M, Muhammad SA. Spatial cluster analysis of human cases of Crimean Congo hemorrhagic fever reported in Pakistan. *Infect Dis Poverty* 4(1):9, 2015.

27. Kulldorff M, Athas WF, Feurer EJ, Miller BA, Key CR. Evaluating cluster alarms: a space-time scan statistic and brain cancer in Los Alamos, New Mexico. *Am J Public Health* 88(9):1377–80, 1998.

28. Huang L, Kulldorff M, Gregorio D. A spatial scan statistic for survival data. *Biometrics* 63(1):109–18, 2007.

29. Rao H, Shi X, Zhang X. Using the Kulldorff's scan statistical analysis to detect spatio-temporal clusters of tuberculosis in Qinghai Province, China, 2009–2016. *BMC Infect Dis* [Internet]. 2017 Dec [cited 2019 Apr 7];17(1). Available from: http://bmcinfectdis.biomedcentral.com/articles/10.1186/s12879-017-2643-y

30. Willis MD, Winston CA, Heilig CM, Cain KP, Walter ND, Mac Kenzie WR. Seasonality of Tuberculosis in the United States, 1993–2008. *Clin Infect Dis* 54(11):1553–60, 2012.

31. RStudio Team. RStudio: Integrated Development Environment for R [Internet]. Viemma, Austria: RStudio, Inc.; 2019. Available from: https://www.R-project.org/

32. Bivand RS, Wong DWS. Comparing implementations of global and local indicators of spatial association. *TEST* 27(3):716–48, 2018.

33. Statistics Bureau Home Page/What is a densely inhabited district? [Internet]. [cited 2021 Oct 6]. Available from: https://www.stat.go.jp/english/data/chiri/did/1-1.html

34. Touray K, Adetifa IM, Jallow A, et al. Spatial analysis of tuberculosis in an Urban West African setting: is there evidence of clustering? *Trop Med Int Health* 15(6):664–72, 2010.

35. Fares A. Seasonality of tuberculosis. *J Global Infect Dis* 3(1):46, 2011.

36. Thorpe LE, Frieden TR, Laserson KF, Wells C, Khatri GR. Seasonality of tuberculosis in India: is it real and what does it tell us? *Lancet* 364(9445):1613–4, 2004.

37. Wacker M, Holick MF. Vitamin D—Effects on Skeletal and Extraskeletal Health and the Need for Supplementation. *Nutrients* 5(1):111–48., 2013

38. Nelson RJ, Demas GE, Klein SL, Kriegsfeld LJ. Seasonal Patterns of Stress, Immune Function, and Disease [Internet]. Cambridge: Cambridge University Press; 2002 [cited 2022 May 28]. Available from: https://www.cambridge.org/core/books/seasonal-patterns-of-stress-immune-function-and-disease/E3B41512025A65BBA2DF8312C439BD2C

39. Manabe T, Takasaki J, Kudo K. Seasonality of newly notified pulmonary tuberculosis in Japan, 2007–2015. *BMC Infect Dis* 19(1):497, 2019.

40. Negin J, Abimbola S, Marais BJ. Tuberculosis among older adults – time to take notice. *Int J Infect Dis* 32:135–7, 2015.

41. Industrial Safety and Health Law.pdf [Internet]. [cited 2022 May 29]. Available from:https://www.ilo.org/dyn/natlex/docs/ELECTRONIC/27779/61989/F332577679/JPN27779.pdf

42. Yoshikawa R, Kawatsu L, Uchimura K, Ohkado A. Delay in health-care-seeking treatment among tuberculosis patients in Japan: what are the implications for control in the era of universal health coverage? *Western Pac Surveill Responses J* 11(2):37-47, 2020.